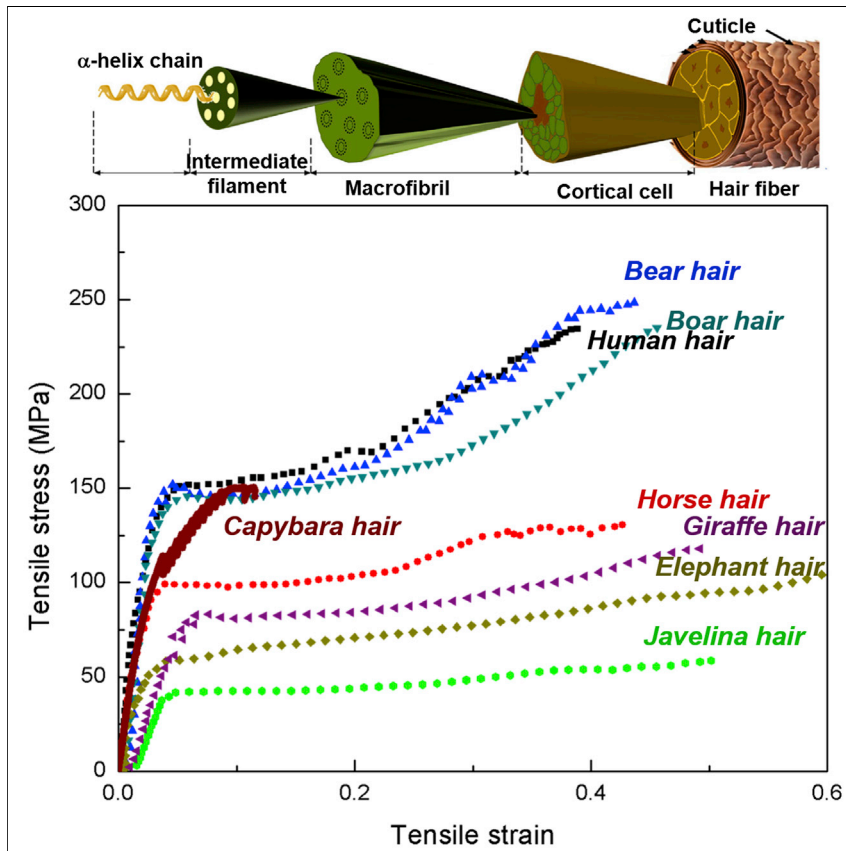


## Article

## On the Strength of Hair across Species



Hair has cosmetic properties but also provides vital protective qualities in many mammals. Thin human hair is strong; 500–1,000 hairs can carry a human weight, whereas thick hair can be relatively weak but displays specific functions, e.g., capybara hair has an oval cross-section with a groove to expedite drying. We find that the tensile strength of hair is increased with decreasing diameter, a mechanical property consistent with Weibull statistics.

Wen Yang, Yang Yu, Robert O. Ritchie, Marc A. Meyers

wyang8207@gmail.com (W.Y.)  
roritchie@lbl.gov (R.O.R.)

## HIGHLIGHTS

Hair consists of hierarchical fibers in a cortex surrounded by cuticle scales

The diameter and structure of hair in mammals can differ due to its functionality

The tensile strength of hair increases with a decrease in its diameter

Inverse dependence of hair strength on size is consistent with Weibull statistics



## Understanding

Dependency and conditional studies on material behavior

## Article

## On the Strength of Hair across Species

Wen Yang,<sup>1,3,\*</sup> Yang Yu,<sup>1</sup> Robert O. Ritchie,<sup>2,\*</sup> and Marc A. Meyers<sup>1</sup>

## SUMMARY

The hair of mammals varies in diameter across species from  $\sim 60\ \mu\text{m}$  in humans to over  $\sim 400\ \mu\text{m}$  in giraffes and elephants. Here, we establish that the tensile strength of hair generally decreases with increasing diameter. Although there is a commonality in the morphology of the hair in such differing species as they all possess a cortex surrounded by cuticles, there are also significant differences in the hierarchical structure that contribute to the observed differences in strength. In this work, the internal structure of the hair from different species is examined, with some unique peculiarities in javelina and capybara hair uncovered. The dimensional dependence of hair strength is compared using Weibull predictions. The good correlation of the strength of hair using such Weibull analysis suggests that the failure strength is dictated by the probability distribution of flaws within the cortex.

## INTRODUCTION

Wool<sup>1–3</sup> and human hair<sup>4–6</sup> are important fibrous keratinous materials that have been widely studied due to their superior mechanical strength and importance in the textile (wool) and hair care industries<sup>7,8</sup> and keratin-based biomaterials fields. In the early 1900s, a patent<sup>9</sup> described a process for extracting keratins from animal horns using lime. The extracted keratins were used to make keratin-based gels that could be strengthened by adding formaldehyde. The technologies were initially applied to animal horns and hooves,<sup>10–15</sup> but were also eventually used to extract keratins from wool and human hair. The biological properties of the extracts led to increased interest in the development of keratins for medical applications, and among the first inventions were keratin powders for cosmetics, composites, and coatings for drugs.<sup>16–18</sup> With modern techniques, fibers mimicking cortex and cuticle structure of hair would be highly attractive. Furthermore, these fibers usually have both protective and defensive functions for their host organism, and thus their mechanical properties, such as their damage and failure mechanisms<sup>19</sup> and constitutive properties,<sup>20</sup> are of considerable significance. When considering their density, which is typically  $\sim 1.3\ \text{Mg m}^{-3}$ , these specific properties can be very impressive. The tensile strength of wool and human hair has been reported to be in the range of 200–260 MPa, yielding a specific (density-normalized) strength of 150–200 MPa/Mg  $\text{m}^{-3}$ , which is on the same order of magnitude as steels and many other metal alloys ( $\sim 250\ \text{MPa/Mg m}^{-3}$ ).

The hierarchical structure of hair is responsible for its mechanical properties.<sup>19,21</sup> The main component of the hair, the inner cortex, is composed of cortical cells (diameter  $\sim 5\ \mu\text{m}$ , length  $\sim 100\ \mu\text{m}$ ) comprising groups of macrofibrils ( $\sim 0.2\text{--}0.4\ \mu\text{m}$  diameter), which in turn consist of intermediate filaments (IFs) (7.5 nm in diameter) embedded in an amorphous matrix. These intermediate filaments are made from  $\alpha$ -helical polypeptide chains. The mechanical properties of hair, its temperature, humidity, and strain-rate sensitivity are the direct result of the interplay between the amorphous and crystalline components of the cortex.<sup>22–25</sup> The keratinous fibers of human hair cortex usually have a large extensibility, with a breaking strain of more than 40%.

## Progress and Potential

Hair provides vital protective qualities in many mammals. Structurally, it consists of a cortex with keratin fibers surrounded by cuticle scales. The exact hair structure, however, can differ in different mammals due to its functionality. For example, as the javelina raises its hair on its back when it is in danger, javelina hair has added stiffness provided by the cellular cortex. The hair of capybara, which is a semi-aquatic animal, has a “twin” structure to create a biconcave cross-section to allow water to be removed easily. In this regard, the diameter of hair varies markedly, from  $\sim 60\ \mu\text{m}$  in humans to over  $\sim 400\ \mu\text{m}$  in giraffes and elephants. Surprisingly, the strength increases with decreasing diameter of the hair, concomitant with a change in fracture path from shear to normal. The relationships between diameter, strength, and failure mechanisms of hair provide insight into how its structure relates to its properties and how this in turn is related to its required functionality.

This large strain to failure is enabled by a plateau in stress, attributed to the unwinding of the  $\alpha$ -keratin structure and, in some cases, to its transformation to  $\beta$ -keratin, which results in an increase in length.<sup>26</sup> Indeed, the total theoretical strain associated with the transformation from  $\alpha$ - to  $\beta$ -keratin in hair is 1.31; one full turn of the helix (0.52 nm) stretches to 1.2 nm in the  $\beta$  configuration. Therefore, several studies have been focused on the mechanical properties and morphologies of keratin fibers,<sup>21,27</sup> in particular to be able to mimic their features in synthetic materials.

The outermost layer of the hair is composed of cuticle scales (0.3–0.5  $\mu\text{m}$  thick and 40–60  $\mu\text{m}$  long) that ensure the integrity of the fibers. These imbricated cuticle scales are found to have a layered structure in human hair. The cuticle consists of layers of scales ( $\sim$ 0.5  $\mu\text{m}$  thickness for each scale) adding to an overall thickness of 2  $\mu\text{m}$ . The keratin is amorphous and does not contain the intermediate filaments of the cortex. The cuticles have a higher sulfur level than the intermediate filaments in the cortex.<sup>28</sup> The cell membrane complex holds all the cuticle cells together and attaches them to the cortex.<sup>6</sup>

Damage to the cuticle, such as after procedures like hair restyling, can cause severe deterioration in mechanical properties principally due to a change of sulfur level, i.e., from the breaking of disulfide bonds, the shaping of the fibers, and subsequent reforming of the disulfide bonds.<sup>29</sup> These chemical bonds, including H bonds and disulfide bonds, are very important to protein (biological) materials, as is evident from several experimental and modeling studies.<sup>30–34</sup> Indeed, such degradation in the mechanical properties of hair is affected not only by the breaking/reforming of disulfide bonds at the nanoscale but also from structural damage to the cuticle and cortex at micro to macro levels, such as hair breakage and split ends due to towel drying, overwashing, and blow-drying wet hair.

Evaluating the mechanical properties of hair is thus of some importance. Previous work has focused on hair from different human races.<sup>35</sup> This particular study found significant variations in the diameter of the hair and in its mechanical properties, which inspired us to investigate the size effect of the hair from different species in nature. Here, we select human (both child and adult), horse, bear, boar, capybara, javelina, giraffe, and elephant hairs to study the relationship between the diameter and mechanical behavior. Our intent is to establish the mechanical properties and toughening mechanisms of hair with different diameters and internal cortex structures. Based on our understanding, we would hope to provide new guidelines for the development of bioinspired synthetic polymeric materials containing both cortex and cuticle.

## RESULTS AND DISCUSSION

### Characterization of the Structure and Fracture Regions

Adult Asian hair with a diameter of 80–100  $\mu\text{m}$  usually is the subject of constant maintenance such as washing with shampoo and conditioner with regular frequency. The surface of the main human hair body usually retains a good quality, exhibiting an undamaged morphology of cuticles, as shown in [Figure 1A](#). The internal component of human hair is the fibrous cortex.<sup>19</sup> After tension testing, the cuticle and the cortex of a human hair were observed to have fractured in different ways: the cuticle usually broke in a brittle mode while the keratinous fibers in the cortex were delaminated in a pull-out mechanism ([Figure 1B](#)). [Figure 1C](#) shows a brittle surface of the cuticle with visualization of the layers, which are assumed to be the overlapped cuticle scales and appear to have a thickness of  $\sim$ 350–400 nm. The observed delamination on the

---

<sup>1</sup>University of California, San Diego, La Jolla, CA 92093, USA

<sup>2</sup>University of California, Berkeley, Berkeley, CA 94720, USA

<sup>3</sup>Lead Contact

\*Correspondence: [wyang8207@gmail.com](mailto:wyang8207@gmail.com) (W.Y.), [roritchie@lbl.gov](mailto:roritchie@lbl.gov) (R.O.R.)

<https://doi.org/10.1016/j.matt.2019.09.019>

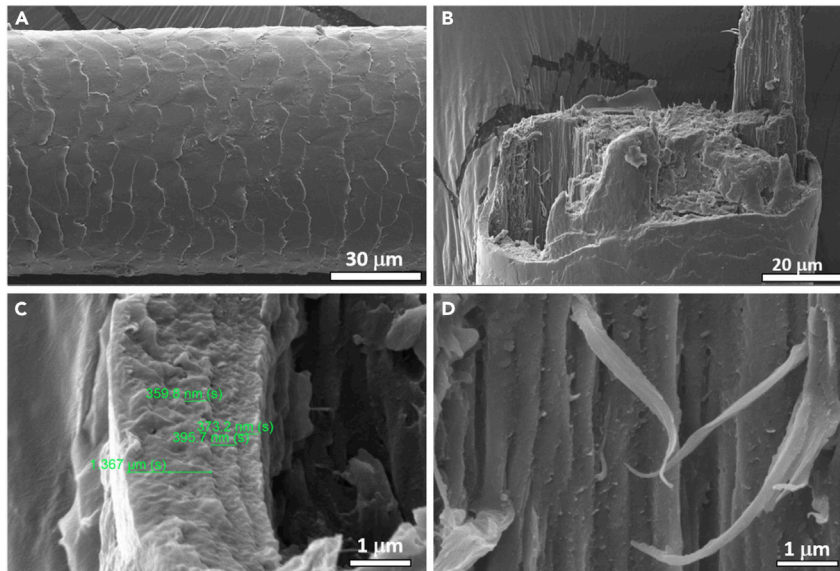


**Figure 1. Human Hair: Morphology, Fracture Surface, and Internal Structure**

- (A) Cuticle arrangement.  
 (B) Fracture of the cortex showing ends of the fibers.  
 (C) Fracture surface of the cuticle showing three layers.  
 (D) Details of the cortex lateral surface showing fiber pull-out.

fracture surface, as well as the brittle nature of this surface, reveal the weak interfacial bonding between the cuticle and cortex and between the fibers in the cortex. Keratinous fibers in the cortex were delaminated and their necking, shown in [Figure 1D](#), indicated that the fibrous cortex is primarily responsible for the mechanical strength of the hair.

The structure of horse hair is similar to human hair except for the diameter, which is some 50% larger (150 versus 100  $\mu\text{m}$ ). In our examination of horse hair, no prior maintenance had been performed except possible washes in river water. Clear damage in the cuticle can be seen in the horse hair ([Figure 2A](#)); many of the scales in cuticle can be seen to be not as closely attached to the body, as in human hair. The fracture of horse hair contains both normal and shear modes. [Figure 2B](#) shows the normal fracture side of the hair after tension with the shear fracture mode on the back side; the cortex fibers were delaminated and peeled off with the fracture of the cuticle. Layers of the cuticle scales were correspondingly exposed, showing the interface between the cuticle and normal fractured cortex ([Figure 2C](#)). Several fibers were pulled out and delaminated at the interface between the cortex and the cuticle; compared with human hair, such fracture surfaces indicate that the horse hair did not experience the same extreme strain as human hair, where the fibers in cortex were pulled out and completely delaminated from the cuticle. Cuticle scales can be seen to have also been lifted off ([Figure 2D](#)), possibly caused by the tensile strains within the horse hair.

Bear hair possesses one of the smallest diameters ( $\sim 80 \mu\text{m}$ ) of the hairs examined, with cuticle scales tightly attached on the body with a certain region of unclear scales (center of the hair in [Figure 3A](#)), which are assumed to be due to caressing by other bears or from the friction between the hairs. Under tensile loading, this hair became split with long cracks created (bottom image in [Figure 3B](#)), indicating that with the

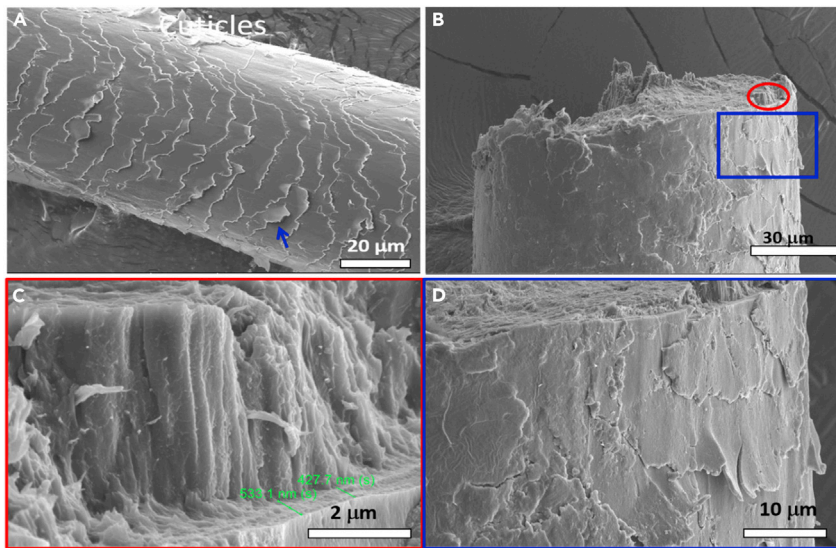


**Figure 2. Surface Morphology and Fracture Surface of Horse Hair**

- (A) Cuticle arrangement, with few scales opening up due to the lack of maintenance.  
 (B) Overview of the normal fracture side.  
 (C) Details of failure surface of cortex; fibers were pulled out such that the thickness of the cuticle can be measured.  
 (D) Details of cuticles showing their elevation.

weak binding effect of the damaged/polished cuticle, the keratinous fibers in the cortex readily delaminated. The delamination of the cortex induces a shear force to the cuticle, which is evident from how the cuticle scales fracture in a zigzag pattern (Figure 3C); this shear force acts to cause the fibers in the cortex to be pulled out (Figure 3D).

Distinct from bear hair, the boar hair is considerably thicker ( $\sim 230 \mu\text{m}$ ) and tends to experience a normal fracture path (perpendicular to the loading direction) under tension (Figure 4A). The exposed cuticle scales are relatively small and, due to the stretching of the edges of the scales, were peeled up from the hair body (Figure 4B). No distinguishing delamination of the fibers was observed at the fracture surface, but one can see that the fibers were bonded tightly in the body of cortex (Figure 4C); only the fibers at the interface between the cortex and cuticle were exposed due to the separation (Figure 4D), which revealed the presence of thick ( $\sim 250 \text{ nm}$  diameter) cortex fibrils. Several were pulled out, as shown in the inserted picture in Figure 4D; these fibrils might serve as a reinforcement for the boar hair.

Similar to the boar hair, juvenile elephant hair is also thick ( $\sim 330 \mu\text{m}$ ; the thickness of mature elephant hair can reach up to  $1.5 \text{ mm}$ ) with an unclear scaled appearance on the surface. It similarly tends to fracture in a normal mode under tension, with the morphology of the fracture surface showing step-like features possibly resulting from the presence of minor defects in the cortex. Some small holes can also be seen on the fracture surface; these were assumed to have originally been the location of the reinforcing fibrils (Figure 5C). Giraffe hair has a comparable diameter with that of the elephant ( $\sim 370 \mu\text{m}$ ), although the arrangement of the cuticle scales is not as clear (Figure 5D) as they are presumed to have been damaged in the environment, e.g., from interactions with trees. However, their fracture mode was similar to that of elephant hairs with the cortex fibrils/fibers again seen to be pulled out from the fracture surface (Figure 5F).

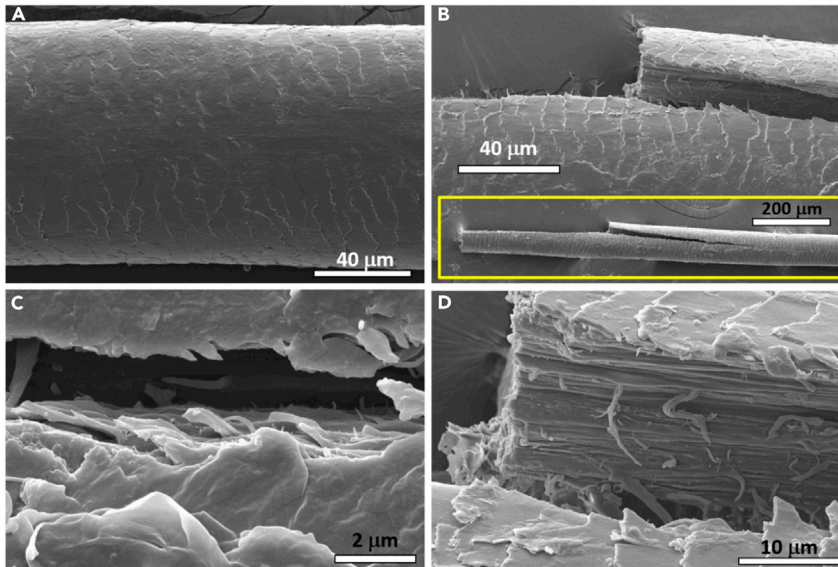


**Figure 3. Surface Morphology, Fracture Surface, and Internal Structure of Bear Hair**

(A) Cuticle arrangement.

(B) Fracture at two points linked to a shear region; note the elevation and fracture of the cuticles.

(C) Cracking in the cuticle with the fibers delaminating in the cortex.

(D) Detailed fibric structure and pull-out of the fibers in the cortex.

Capybara and javelina hairs have quite different structures from the other hairs examined. The capybara hair has a “twin” configuration with an oval-like shape (Figure 6A); scales can be seen on the surface of cuticle with a slight sulcus between the “twins.” This specific structure provides a path for water dripping from the hair and the exposure of large area to the wind and the sun for rapid drying. Under tension, cracks prefer to separate the “twins” and each twin tends to fail by shear fracture (Figure 6B), such that many of the cortex fibers delaminate and are pulled out by the shear force (Figures 6C and 6D). The javelina hair has a porous cortex, and the cuticle layer does not show clear scales. This structure is similar to that of American porcupine quills,<sup>36,37</sup> yet the javelina hair has a much smaller diameter ( $\sim 300 \mu\text{m}$ ). The cortex contains closed cells with a size of  $10\text{--}30 \mu\text{m}$  (Figure 7B); stiffeners with a fibrous structure connect to the cellular structure. The cell wall has a porous layered structure with the pore size of  $0.5\text{--}3 \mu\text{m}$  (Figure 7D); these layers are formed by keratinous fibers (Figure 7C). Without the support of the fibrous cortex, the cuticle cracks in a shear path (Figure 7A), with only the fibers in the stiffeners pulled out and slightly delaminated under tension; such a structure is designed to maximize stiffness, with the hair in the neck standing up, increasing its size in a virtual manner, possibly as a defense mechanism by the javelina against predators. The interfaces between cells, as well as the cell walls and stiffeners, can accommodate energy dissipation<sup>36,37</sup> under compression but are relatively weak under tension.

### Mechanical Behavior of Hair from Different Species

Significant differences were observed in the tensile response of hair from the differing species, as shown by their characteristic stress-strain curves in Figure 8. Human, horse, boar, and bear hair have a mechanical response similar to that of wool.<sup>38</sup> With their relatively high elastic modulus of  $\sim 3.5\text{--}5 \text{ GPa}$ , the curves consist of a linear (elastic) region followed by a plateau with slowly rising stress up to a strain of  $0.20\text{--}0.25$  before the hardening rate increases significantly up to a failure strain of

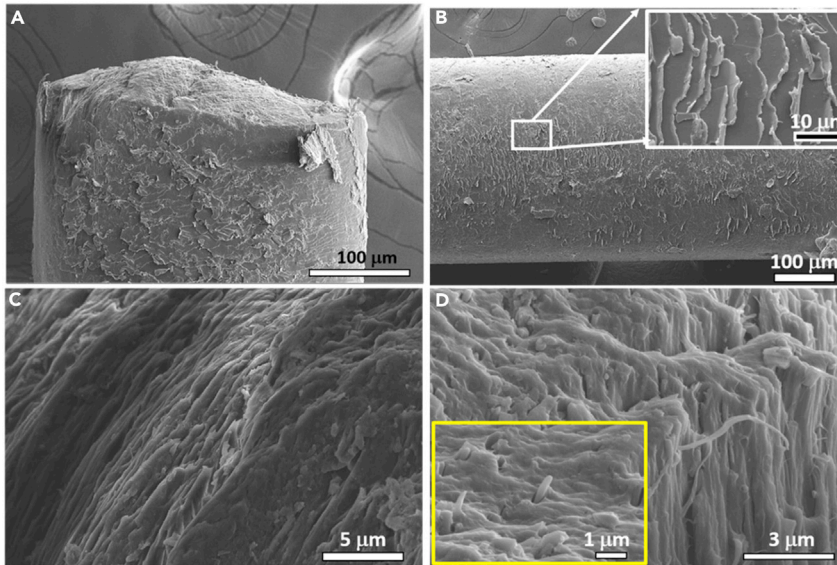


**Figure 4. Surface Morphology and Fracture Surface of Boar Hair**

- (A) Flat normal fracture.  
 (B) Cuticle arrangement showing the poor state of preservation of the cuticle scales.  
 (C) Details at the interface between the cortex and cuticle on the fracture surface.  
 (D) Pulled-out fibers and protruding fibrils.

$\sim 0.40$ . The plateau region is attributed to the unwinding of the  $\alpha$ -helical structure of keratin intermediate filaments which, in some cases, can transform (partially) to  $\beta$  sheets; the complete unwinding generates a strain of 1.31,<sup>19</sup> much higher than the one at the end of this stage (0.20–0.25). The crystalline filamentary part of the structure is surrounded by the amorphous matrix, which does not transform; this amorphous region corresponds to  $\sim 55\%$  of the total, assuming that the diameter of intermediate filaments is 7 nm and that they are separated by 2 nm of amorphous material (these measurements were deduced from the results of Yu et al.<sup>19</sup>). At the stage of deformation characterized by hardening, sliding between the cortical fibers takes place, as well as between the smaller structural elements such as the microfibrils, intermediate filaments, and amorphous matrix.

The giraffe, elephant, and javelina hairs have an approximate linear hardening response without a clear distinction between the plateau and rapid hardening regions. The elastic modulus is relatively low,  $\sim 2$  GPa. In contrast to the other species, the capybara hair exhibits a response characterized by rapid hardening upon which sequential load drops are superimposed. The load drops correspond to the sliding between the “twin” strands in the capybara hair; moreover, the maximum strain is much lower than for the other keratinous hairs ( $\sim 0.1$ ). The capybara is a semi-aquatic animal, and the specific shape of the hair is hypothesized to be related to allowing water droplets to exit faster. It is also possible that the mechanical properties with such a structure are less influenced by hydration.

The decrease in Young’s modulus with increasing diameter of the various species of hair was previously reported by Yu et al.,<sup>20</sup> who also noted that the elastic modulus of the javelina hair was significantly lower than the other hairs because of its inner porosity, shown in Figure 7. The javelina hair has both black and white segments, with failure usually occurring in the white segments; the darker hair has greater strength due to the melanosomes, which are only found in black hair.<sup>39</sup>

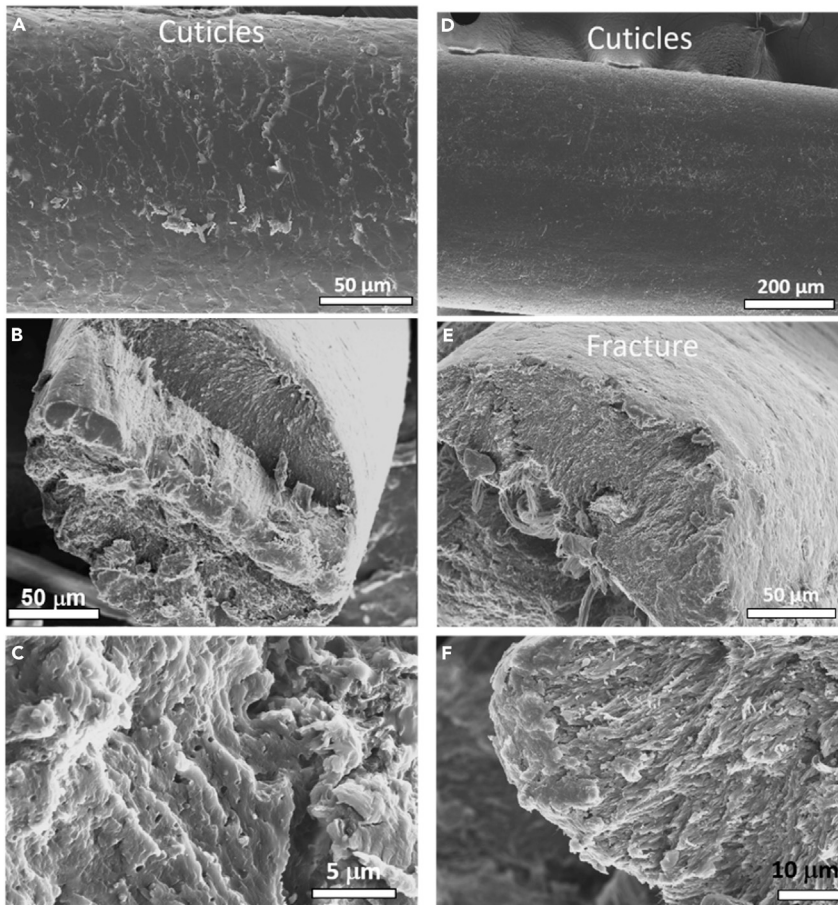


**Figure 5. Surface Morphology and Fracture Surface of Elephant and Giraffe Hair**

(A–C) Elephant hair. (A) Cuticle arrangement. (B) Step-case surface with a high potential for normal fracture (not a shear fracture), (C) Hollow channels on the fracture surface indicating where the fibrils were pulled out.

(D–F) Giraffe hair. (D) Unclear cuticle scales. (E) Normal fracture surface. (F) Fibers pulled out from the fracture surface.

### Size Effect on the Strength of Hair

The diameter of mammalian hair is significantly dependent on species, as indicated in [Figure S1](#), which shows the variation in diameter of the hairs. The diameter of the scales, in general, vary with the size of the animal. These results were obtained from three measurements made at each location by rotating the hair, with more measurements performed at the location where there was a greater variation in diameter. Certain conclusions can be drawn by these measurements. (1) In terms of the variation along a single hair, most hairs have a certain consistency of thickness in their central region with a decrease in thickness at the tip; the hair of wild animals appears to have a little more variation in thickness due to their growth and living environments. (2) For the variation in diameter between hairs within one species, most hairs align within a similar range of diameters for a single type of animal. The hair from different animals in one species can vary, but we have no information about this issue as we do not know whether the hair that we examined came from one or more individual animals. (3) For the hair of different mammals, a clear distinction in the diameter of the hairs can be seen. As such, we were able to obtain the relationship between breaking stress and average diameter, as shown in



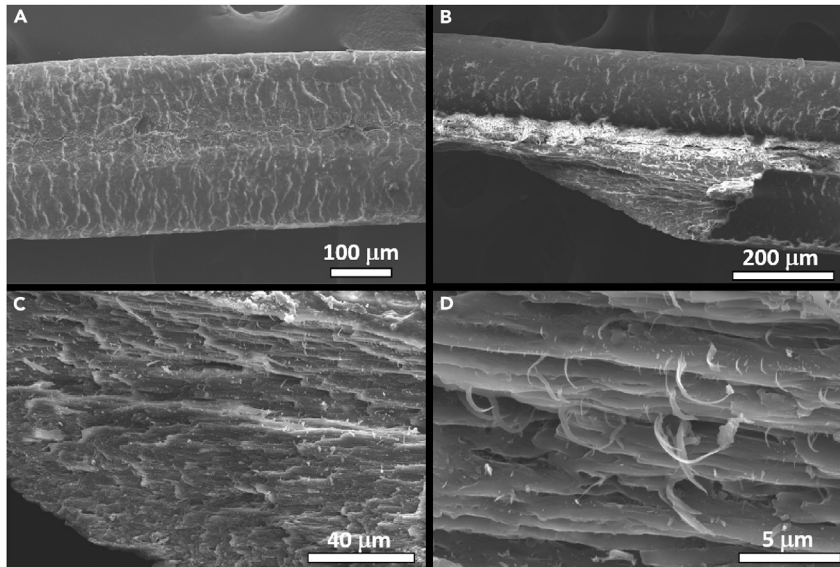


**Figure 6. Surface Morphology and Fracture Surface of Capybara Hair**

- (A) Cuticle arrangement and “twins” appearance.  
 (B) Shear fracture of one twin hair.  
 (C) Fibers close to the boundary appear brittle and stiff.  
 (D) Fibers were pulled out on the fracture surface of the twin hair.

Figure 9; here the samples for the Weibull analysis were carefully selected at a thickness with little variation.

Due to the variation in the diameter and tensile properties of the hairs, it is interesting to determine whether their breaking stresses can be predicted from Weibull statistics,<sup>40</sup> which can specifically take account of differences in sample size and the resulting flaw size.

A hair segment, with a volume  $V$ , is assumed to be made up of  $n$  volume elements, with each unit volume  $V_0$  possessing a similar flaw distribution. Using a weakest-link assumption, at a given stress level  $\sigma$ , the probability  $P$  of survival of a given hair segment with volume  $V$  can be expressed as the product of the incremental survival probabilities of each of the volume elements, namely:

$$P(V) = P(V_0) \cdot P(V_0) \cdot \dots \cdot P(V_0) = P(V_0)^n, \quad (\text{Equation 1})$$

where the volume  $V$  comprises  $n$  volume elements  $V_0$ . As the stress increases,  $P(V)$  naturally decreases. Using the Weibull (two-parameter) representation of this weakest-link concept, the probability of failure of the entire volume can be expressed as:

$$1 - P(V) = 1 - \exp\left[-\frac{V}{V_0} \left(\frac{\sigma}{\sigma_0}\right)^m\right], \quad (\text{Equation 2})$$

where  $\sigma$  is the applied stress,  $\sigma_0$  is a characteristic (reference) strength, and  $m$  is the Weibull modulus, which is a measure of the variability in properties. It can be seen that the probability of failure increases with increase in the sampling volume  $V$  at a constant stress  $\sigma$ . Figure 9A shows the Weibull distribution of experimental breaking stresses for the human and capybara hair. The curves for the other species were predicted using Equation 2 with the same  $m$  value as for human hair ( $m = 0.11$ ). Due to the lack of large amounts of hair from other species, the ratio of their volume per unit length to the volume of human hair per unit length,  $(V/V_0)$ , was taken for the

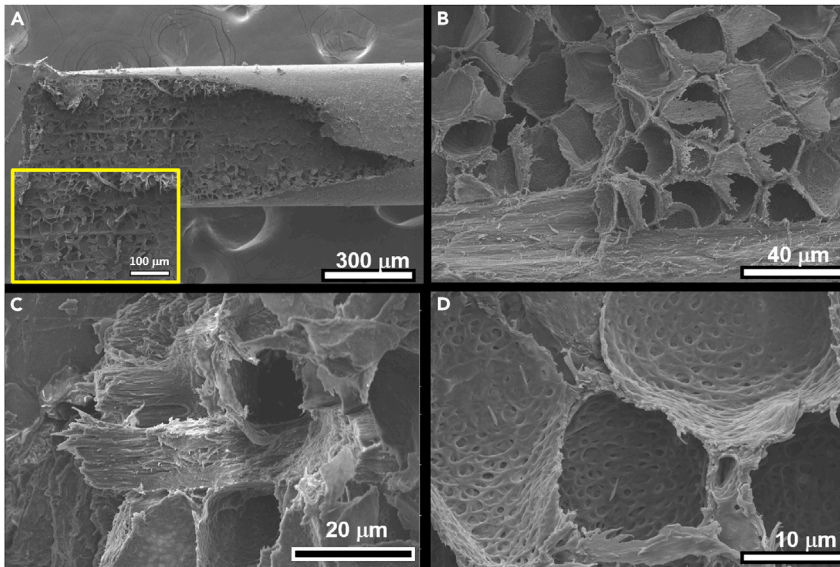


**Figure 7. Surface Morphology and Fracture Surface of Javelina Hair**

- (A) Cuticle arrangement and the fracture surface.  
 (B) General morphology of the cortex failure showing the alignment of features.  
 (C) Closed cells (cell diameter  $\sim 20 \mu\text{m}$ ) with cell walls composed of fibers.  
 (D) Higher magnification of cell walls.

calculation of the predicted curves. The average hair diameters used were boar hair  $\sim 235 \mu\text{m}$ , horse hair  $\sim 200 \mu\text{m}$ , javelina hair  $\sim 300 \mu\text{m}$ , bear hair  $\sim 70 \mu\text{m}$ , elephant hair  $\sim 345 \mu\text{m}$ , and giraffe hair  $\sim 370 \mu\text{m}$ . Based on the notion that the breaking stress can be defined at  $P(V) = 0.5$ , these results indicate that the breaking stress decreases with increasing hair diameter across the various species.

Figure 9B shows both the predicted breaking stresses at 50% probability of failure ( $P(V) = 0.5$ ) and average experimental breaking stress (with error bars) for the different species. It is clear that as the hair diameter increases from  $\sim 100 \mu\text{m}$  to  $\sim 350 \mu\text{m}$ , its breaking stress decreases from  $\sim 200\text{--}250 \text{MPa}$  to  $\sim 125\text{--}150 \text{MPa}$ . Predictions based on Weibull analysis agree well with the experimental data, except for the javelina hair, which as discussed earlier is highly porous. Its strength is lower than the Weibull prediction.

Consistent with the results reported here, wool is known to have a breaking stress ( $\sim 260 \text{MPa}$ ) that slightly exceeds human hair<sup>38</sup> as it has a smaller diameter of  $20\text{--}80 \mu\text{m}$ . Moreover, it has been reported that beard hair, which invariably displays a larger diameter than head hair, exhibits lower breaking stress.<sup>40</sup> Both these examples of wool and beard hair fit well with our data on breaking stresses as a function of average diameter.

From a perspective of fracture modes, the morphologies of the failure of our hair samples, at a strain rate of  $10^{-2} \text{s}^{-1}$ , suggest that those with a diameter less than  $\sim 200 \mu\text{m}$  tend to fracture in a shear mode, whereas the hair with a larger diameter, exceeding  $\sim 200 \mu\text{m}$ , tends to fail in a normal tensile mode. We presume that this effect is related to the size of the flaw in relation to the hair diameter. If the ratio between these two length scales is large, a state of uniaxial tension is generated but with the maximum shear stress dominating the failure. If the flaw is small with respect to the diameter, the stress state is dominated by the tensile stresses, which

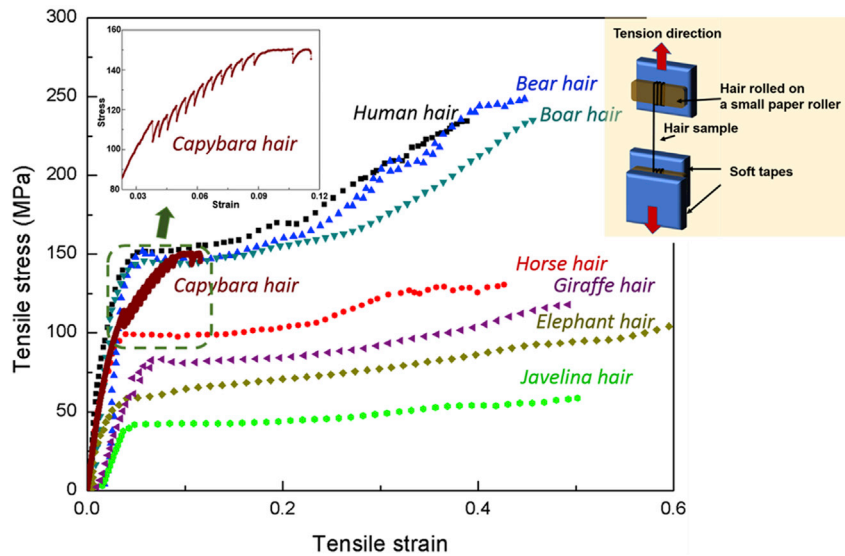


**Figure 8. Typical Uniaxial Engineering Stress-Strain Curves of Different Types of Hair with the Schematic Drawing of Mounted Hair Sample Shown on the Top Right, at a Strain Rate of  $10^{-2} \text{ s}^{-1}$**   
 Human and bear hairs are the strongest, exhibiting a plateau-like response followed by higher strain hardening. Javelina hair is at the opposite end of the spectrum by virtue of its cellular structure. Horse, giraffe, and elephant hairs show a quasi-linear hardening. Capybara hair is atypical, showing serrations and a much more pronounced strain hardening.

favor a normal fracture path. This is analogous to the change in failure morphology in metals when the sample thickness increases, from a shear to a normal mode, for plane stress versus plane strain configurations, respectively.

## Conclusions

An experimental study has been carried out on the structure and mechanical properties of mammalian hair from eight species: human (child and adult), horse, bear, boar, javelina, capybara, elephant, and giraffe. Based on this work, the following conclusions can be made.

1. Similarities between the structure of the hair from different species are clearly evident; specifically, the principal structural features common to these mammals are the inner cortex, which is composed of crystalline fibers embedded in an amorphous matrix, and an outer cuticle layer consisting of overlapping scales. The cortex is composed of fibers and is responsible for the tensile strength while the primary function of the cuticles is to ensure the integrity of hair.
2. The hair of the javelina, however, is somewhat different, presumably due to its role in the defense of the animal. The cortex in the javelina hair consists of a closed-cell foam structure similar to that in American porcupine quills, instead of the fibrillar structure of the other hairs.
3. There is a clear correlation between diameter and the tensile strength of the hair, the strength decreasing with increasing hair diameter, concomitant with a change in fracture path from a shear to a normal mode. These experimental results are consistent with weakest-link statistical predictions and confirm the Weibull hypothesis of a flaw-determined fracture in hair.
4. The mechanical response of hair is characterized as a linear elastic region followed by a plateau with moderate strain hardening and, in the case of human,

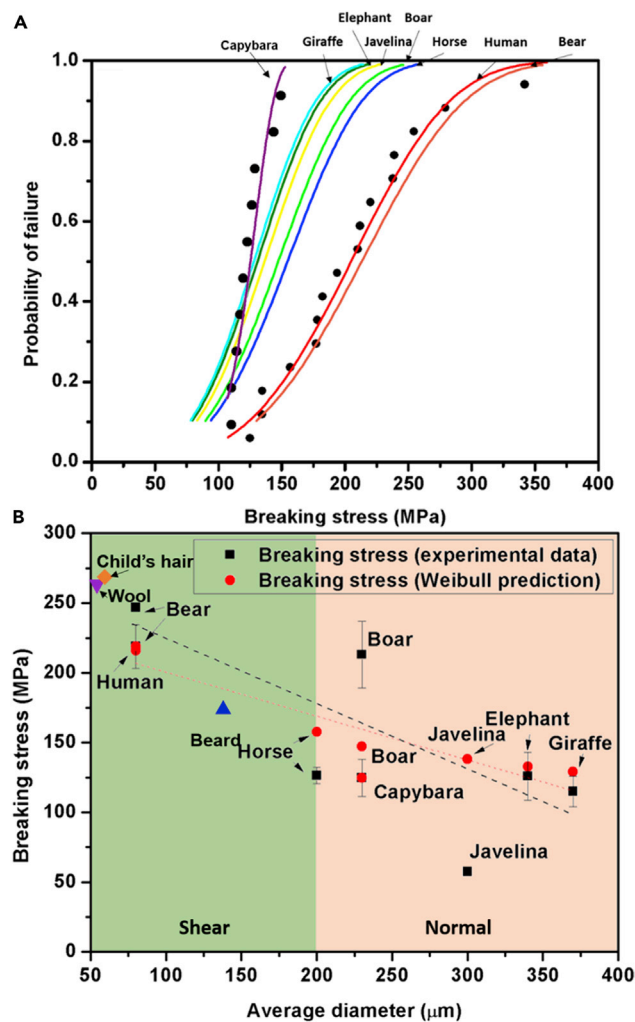


**Figure 9. Statistical Breaking Strengths of Hairs in Relation to Their Diameter**

(A) Experimentally measured and predicted Weibull probability of the failure stress for hair from differing species with varying diameter.

(B) Experimentally obtained (dashed line) and Weibull predictions (for  $P(V) = 0.5$ , dotted line) of these failure stresses for hair from eight species. Data for wool and beard were collected from Feughelman<sup>3</sup> and Thozhur et al.<sup>41</sup>

boar, and bear hair, a stage with a much larger hardening rate. This plateau is attributed to the unwinding of the helical coils in the  $\alpha$ -keratin followed by their transformation to  $\beta$  sheets. It is known that this transformation, if completed, generates a strain of 1.3 in the crystalline component of the cortex. The fact that the plateau reaches a level of strain of only 0.2–0.25 suggests that the unwinding of the  $\alpha$ -keratin coils partially happens.

## EXPERIMENTAL PROCEDURES

### Sources of Hair

For our experiments, human hair specimens were obtained from two East-Asian females, a 30-year-old adult and a 9-year-old child. No additional chemical treatments (such as permanent waving and dyeing) other than shampooing had been performed on the hair. Horse hairs were procured from the tail of a 16-year-old Arabian gelding; these were rinsed to remove dirt and subsequently kept under

ambient conditions for over 24 h to remove the extra moisture. Asian elephant and giraffe tail hairs were obtained from QinLing Safari Park (Xi'an, China), whereas hairs from the boar, javelina, and bear were provided by local hunters. Capybara hair was obtained from a specimen on the Paraguay River, Brazil. Hair from a mature African elephant was obtained from Cape Town University.

### Specimen Preparation and Mechanical Testing

The ends (~20 mm) of all hair specimens were first trimmed off to exclude the influences of property changes at tip and root ends.<sup>24</sup> Sections with a length of ~30 mm were separated to prepare the tensile samples. Both ends were tied to small paper rolls (~3 mm diameter) and glued to tape segments, leaving approximately 10 mm in the middle region as the gauge length (this is shown in the schematic drawing at the top right-hand side of [Figure 8](#)); some types of hair, however, were not sufficiently long such that their gauge lengths were correspondingly shorter. This setup ensured that the hair fractured in the center of each sample without slipping from the tension grips at the ends. Most hairs generally have a cylindrical shape, but some regions show an elongated cross-section. We calculated from our measurements the eccentricity along the hairs and determined the largest eccentricity,  $e = \sqrt{1 - \frac{b^2}{a^2}}$  (not including the hair tip), where  $a$  is the length of semi-major axis and  $b$  is the length of semi-minor axis for each type of hair. Specifically, these measurements yielded the following maximum eccentricity values: child = 0.18, adult = 0.49, bear = 0.65, horse = 0.62, boar = 0.79, javelina = 0.59, and giraffe = 0.66. The tensile strength of tested hair samples with a distinct eccentricity was computed using the elliptical cross-section area ( $A = \pi ab$ ); for example, this was the case for the capybara hair. Additional measurements on each type of hair are provided in [Figure S1](#). At least nine measurements were made using a micrometer on each sample within the tested length (10 mm) at three positions (three measurements at one position by rotating the hair) before testing. The average value was used for the diameter in the data analysis. To ensure data accuracy, from the perspective of discerning the general strength of hair and how this strength may vary between different species, we confined all the samples that were selected for testing to within a certain diameter range for that species.

Uniaxial tension tests were conducted on an Instron 3342 universal testing system equipped with a 500 N load cell at a strain rate of  $10^{-2} \text{ s}^{-1}$ . At least 3–5 samples were tested for each species.

### Characterization of Original Structures and Damaged Surfaces

To compare the morphology of the hairs before and after tensile extension, we performed characterization of the cuticle and fracture surface using scanning electron microscopy on an FEI Quanta 250 scanning electron microscope and an FEI Apreo scanning electron microscope (FEI, Hillsboro, OR). Samples were carefully prepared and sputtered with iridium prior to imaging.

### SUPPLEMENTAL INFORMATION

Supplemental Information can be found online at <https://doi.org/10.1016/j.matt.2019.09.019>.

### ACKNOWLEDGMENTS

This work was supported by the Multidisciplinary University Research Initiative to the University of California, Riverside, funded by the Air Force Office of Scientific Research (AFOSR-FA9550-15-1-0009), with subcontracts to UC San Diego and UC

Berkeley. Additionally, Y.Y. was supported by the Powell Foundation through the Jacobs School of Engineering at UCSD. We appreciate the help given by Nancy Guo in procuring the elephant and giraffe hairs and the Norbert and Betsy Schultz family in procuring the bear, boar, and javelina hairs. We thank Alexandria Do for help with the thickness measurements of the hair.

## AUTHOR CONTRIBUTIONS

W.Y. and Y.Y. performed the experiments. W.Y., M.A.M., and R.O.R. wrote the manuscript.

## DECLARATION OF INTERESTS

The authors declare no competing interests.

Received: July 7, 2019

Revised: September 5, 2019

Accepted: September 23, 2019

Published: January 8, 2020

## REFERENCES

- Crewter, W.G. (1972). The effects of disaggregating agents on the stress-strain relationship for wool fibers. *Text. Res. J.* 42, 77–85.
- Chapman, B.M. (1969). A mechanical model for wool and other keratin fibers. *Text. Res. J.* 39, 1102–1109.
- Feughelman, M. (1997). *Mechanical Properties and Structure of Alpha-Keratin Fibres: Wool, Human Hair and Related Fibres* (UNSW Press).
- Dankovich, T.A., Kamath, Y.K., and Ruetsch, S. (2004). Tensile properties of twisted hair fibers. *J. Cosmet. Sci.* 55, S79–S90.
- Scott, G.V., and Robbins, C.R. (1978). Stiffness of human hair fibers. *J. Soc. Cosmet. Chem.* 29, 469–485.
- Seshadri, I.P., and Bhushan, B. (2008). In situ tensile deformation characterization of human hair with atomic force microscopy. *Acta Mater.* 56, 774–781.
- Wang, B., Yang, W., McKittrick, J., and Meyers, M.A. (2016). Keratin: structure, mechanical properties, occurrence in biological organisms, and efforts at bioinspiration. *Prog. Mater. Sci.* 76, 229–318.
- McKittrick, J., Chen, P.Y., Bodde, S.G., Yang, W., Novitskaya, E.E., and Meyers, M.A. (2012). The structure, functions, and mechanical properties of keratin. *JOM* 64, 449–468.
- Hofmeier, J. (1905). Horn-lime plastic masses from keratin substances. German Patent DE184915.
- Breidl, F., and Baudisch, O. (1907). The oxidative breaking up of keratin through treatment with hydrogen peroxide. *Z. Physiol. Chem.* 52, 158–169.
- Neuberg, C. (1909). Process of producing digestible substances from keratin. US Patent 926,999.
- Lissizin, T. (1915). Behavior of keratin sulfur and cystin sulfur in the oxidation of these proteins by potassium permanganate I. *Biochem. Bull.* 4, 18–23.
- Zdenko, S. (1924). Solubility and digestibility of the degradation products of albumoids I. *Z. Physiol. Chem.* 136, 160–172.
- Lissizin, T. (1928). The oxidation products of keratin by oxidation with permanganate II. *Z. Physiol. Chem.* 173, 309–311.
- Goddard, D.R., and Michaelis, L. (1935). Derivatives of keratin. *J. Biol. Chem.* 112, 361–371.
- Beyer, C. (1907). The keratin or horny substance of the hair. German Patent DE22643.
- Dale, H.N. (1932). Keratin and other coatings for pills. *Pharm. J.* 129, 494–495.
- Rouse, J.G., and Van Dyke, M.E. (2010). A review of keratin-based biomaterials for biomedical applications. *Materials (Basel)* 3, 999–1014.
- Yu, Y., Yang, W., Wang, B., and Meyers, M.A. (2017a). Structure and mechanical behavior of human hair. *Mater. Sci. Eng. C* 73, 152–163.
- Yu, Y., Yang, W., and Meyers, M.A. (2017b). Viscoelastic properties of  $\alpha$ -keratin fibers in hair. *Acta Biomater.* 64, 15–28.
- Velasco, M.V., Dias, T.C., Freitas, A.Z., Júnior, N.D., Pinto, C.A., Kaneko, T.M., and Baby, A.R. (2009). Hair fiber characteristics and methods to evaluate hair physical and mechanical properties. *Braz. J. Pharm. Sci.* 45, 153–162.
- Nikiforidis, G., Balas, C., and Tsambaos, D. (1992). Viscoelastic response of human hair cortex. *Med. Biol. Eng. Comput.* 30, 83–88.
- Barnes, H.A., and Roberts, G.P. (2000). The non-linear viscoelastic behaviour of human hair at moderate extensions. *Int. J. Cosmet. Sci.* 22, 259–264.
- Robinson, M.S., and Rigby, B.J. (1985). Thiol differences along keratin fibers: stress/strain and stress-relaxation behavior as a function of temperature and extension. *Text. Res. J.* 55, 597–600.
- Rebenfeld, L., Weigmann, H.D., and Dansizer, C. (1966). Temperature dependence of the mechanical properties of human hair in relation to structure. *J. Soc. Cosmet. Chem.* 17, 525–538.
- Kreplak, L., Doucet, J., Dumas, P., and Briki, F. (2004). New aspects of the  $\alpha$ -helix to  $\beta$ -sheet transition in stretched hard  $\alpha$ -keratin fibers. *Biophys. J.* 87, 640–647.
- Swift, J.A. (1999). Human hair cuticle: biologically conspired to the owner's advantage. *J. Cosmet. Sci.* 50, 23–48.
- Birbeck, M.S.C., and Mercer, E.H. (1957). The electron microscopy of the human hair follicle: part 3. The inner root sheath and trichohyaline. *J. Biophys. Biochem. Cytol.* 25, 223–230.
- Popescu, C., and Höcker, H. (2007). Hair—the most sophisticated biological composite material. *Chem. Soc. Rev.* 36, 1282–1291.
- Fratzl, P., and Weinkamer, R. (2007). Nature's hierarchical materials. *Prog. Mater. Sci.* 52, 1263–1334.
- Fratzl, P., Gupta, H.S., Paschalis, E.P., and Roschger, P. (2004). Structure and mechanical quality of the collagen-mineral nano-composite in bone. *J. Mater. Chem.* 14, 2115–2123.
- ZhiMing, Y., Bo, K., XiaoWei, H., ShaoLei, L., YouHuang, B., WoNa, D., Ming, C., Hyung-Taeg, C., and Ping, W. (2011). Root hair-specific expansions modulate root hair elongation in rice. *Plant J.* 66, 725–734.
- Qin, Z., Cranford, S., Ackbarow, T., and Buehler, M.J. (2009). Robustness-strength performance of hierarchical alpha-helical protein filaments. *Int. J. Appl. Mech.* 1, 85–112.

34. Cranford, S.W., and Buehler, M.J. (2013). Critical cross-linking to mechanically couple polyelectrolytes and flexible molecules. *Soft Matter* **9**, 1076–1090.
35. Franbourg, A., Hallegot, P., Baltenneck, F., Toutaina, C., and Leroy, F. (2003). Current research on ethnic hair. *J. Am. Acad. Dermatol.* **48**, S115–S119.
36. Yang, W., Chao, C., and McKittrick, J. (2013a). Axial compression of a hollow cylinder filled with foam: a study of porcupine quills. *Acta Biomater.* **9**, 5297–5304.
37. Yang, W., and McKittrick, J. (2013b). Separating the influence of the cortex and foam on the mechanical properties of porcupine quills. *Acta Biomater.* **9**, 9065–9074.
38. Fraser, R.D.B., and MacRae, T.P. (1980). Molecular structure and mechanical properties of keratins. In *The Mechanical Properties of Biological Materials*, J.F.V. Vincent and J.D. Currey, eds. (Cambridge University Press), pp. 211–246, (Proc. Symposia of the Society for Experimental Biology).
39. Oresajo, C., and Pillai, S. (2007). Black skin cosmetics: specific skin and hair problems of African Americans and cosmetic approaches for their treatment. In *Ethnic Skin and Hair*, E. Berardesca, J.L. Leveque, and H.I. Maibach, eds. (CRC Press), p. 205.
40. Weibull, W. (1951). A statistical distribution function of wide applicability. *J. Appl. Mech.* **18**, 293–297.
41. Thozhur, S.M., Crocombe, A.D., Smith, P.A., Cowley, K., and Mullier, N. (2006). Structural characteristics and mechanical behaviour of beard hair. *J. Mater. Sci.* **41**, 1109–1121.